Time-Frequency Representations as Phase Space Reconstruction in Symbolic Recurrence Structure Analysis

Mariia Fedotenkova, Peter Beim Graben, Jamie Sleigh, Axel Hutt

▶ To cite this version:

HAL Id: hal-01415997
https://hal.archives-ouvertes.fr/hal-01415997

Time-Frequency Representations as Phase Space Reconstruction in Symbolic Recurrence Structure Analysis

Mariia Fedotenkova[1,2,3], Peter beim Graben[4], Jamie W. Sleigh[5] and Axel Hutt[6]

[1] NEUROSYS team, INRIA, Villers-lès-Nancy, F-54600, France
[2] UMR n° 7503, CNRS, Loria, Vanduvre-lès-Nancy, F-54500, France
[3] Université de Lorraine, Villers-lès-Nancy, F-54600, France
[4] Bernstein Center for Computational Neuroscience, Berlin, Germany
[5] Waikato Clinical School of the University of Auckland, New Zealand
[6] Deutscher Wetterdienst, Offenbach am Main, Germany
maria.fedotenkova@gmail.com

Abstract. Recurrence structures in univariate time series are challenging to detect. We propose a combination of symbolic and recurrence analysis in order to identify recurrence domains in the signal. This method allows to obtain a symbolic representation of the data. Recurrence analysis produces valid results for multidimensional data, however, in the case of univariate time series one should perform phase space reconstruction first. In this chapter, we propose a new method of phase space reconstruction based on signal's time-frequency representation and compare it to the delay embedding method. We argue that the proposed method outperforms the delay embedding reconstruction in the case of oscillatory signals. We also propose to use recurrence complexity as a quantitative feature of a signal. We evaluate our method on synthetic data and show its application to experimental EEG signals.

Keywords: recurrence analysis, symbolic dynamics, time-frequency representation, Lempel-Ziv complexity, EEG

1 Introduction

Recurrent temporal dynamics is a phenomenon frequently observed in time series measured in biological systems. For instance, bird songs exhibit certain temporal structures, that recur in time [28]. Other examples are returning epileptic seizures [2], recurrent brain microstates in language processing [3] and in early auditory neural processing [14]. All these latter phenomena are observed in electroencephalographic data (EEG). To detect such temporal recurrent structures, typically one applies recurrence analysis [5, 21] based on Poincaré's theorem [24]. This approach allows the detection of recurrence structures in multivariate time series. To retrieve recurrence structures from univariate time, several methods have been suggested, such as delay embedding techniques.

However, most existing methods do not take into account specifically the oscillatory nature of the signals as observed in biological systems. To this end, we propose a technique to embed the univariate time series in a multidimensional space to better consider oscillatory activity. The approach is based on the signals time-frequency representation. In a previous work we have sketched this approach [27] already but without discussing its performance subject to different time-frequency representations. The present work shows this detailed discussion and suggests a new method to classify signals according to their recurrence complexity. Applications to artificial data permits to evaluate the method and compare it to results gained from the conventional delay embedding technique. Final applications to experimental EEG data indicates the method's future application.

2 Analysis Methods and Data

2.1 Symbolic Recurrence Structure Analysis

Recurrence is a fundamental property of nonlinear dynamical systems, which was first formulated by Poincaré in [24]. It was further illustrated in recurrence plot (RP) technique proposed by Eckmann et al. [5]. This relatively simple method allows to visualize multidimensional trajectories on a two-dimensional graphical representation. The RP can be obtained by plotting the recurrence matrix:

$$R_{ij} = \Theta \left(\varepsilon - ||\boldsymbol{x}_i - \boldsymbol{x}_j|| \right), \qquad i,j = 1, 2, \ldots, N \ , \tag{1}$$

where $\boldsymbol{x}_i \in \mathbb{R}^d$ is the state of the complex system in the phase space of dimension d at a time instance i; $|| \cdot ||$ denotes a metric, Θ is the Heaviside step function, and ε is a threshold distance.

It can be seen from (1), that if two points in the phase space are relatively close, the corresponding element of the recurrence matrix $R_{ij} = 1$, which would be represented by a black dot on the RP.

Instead of analyzing RPs point-wise we concentrate our attention on recurrence domains, labeling each domain with a symbol, thus obtaining recurrence plots of symbolic dynamics. The RP from symbols were successfully used in several studies (see, for instance, [6, 17, 4]). Here, we use symbolic recurrence structure analysis (SRSA) proposed in [11], this technique allows to obtain symbolic representations of the signal from the RP, the latter being interpreted as a set of rewriting rules. According to these rules, large time indices are substituted with smaller ones when two states, occurring at these times, are recurrent. The process starts by initializing a symbolic sequence with discrete time at which the signal is computed, i.e., $s_i = i$. Next, this sequence is recursively rewritten based on the elements in the RP, namely, $s_i \rightarrow s_j$ if $i > j$ and $R_{ij} = 1$. Afterwards, the sequences is scanned for monotonically increasing indices and each of them is mapped to one symbol $s_i = 0$, which labels transient states. This is done to differentiate between metastable states from transitions between them. More detailed description of the method and examples can be found in [11, 12].

By examining (1) one can see that the resulting recurrence matrix and, thus, symbolic sequence strongly depend on distance threshold parameter ε. Several techniques for optimal ε estimation exist [22], most of which are heuristic. SRSA aims to obtain an optimal value of ε from the data.

Here, we propose two approaches to estimate ε optimally, based on (i) the principle of maximal entropy and (ii) Markov chain model of the system. The former implies that the system spends an equal amount of time in each recurrence domain [11], while the latter takes into account the probabilities of the system's transition from one recurrence state to another [12]. Each of these approaches assumes a certain model for the system's dynamics, hence for each ε value we can calculate a value of a utility function, which describes how well an obtained symbolic sequence fits to the proposed model. The optimal value of the threshold distance ε^* will then be the one to maximize the value of the utility $u(\varepsilon)$ function:

$$\varepsilon^* = \arg \max_{\varepsilon} u(\varepsilon) \ . \tag{2}$$

The utility function is different for both models. In the first case, the utility function is presented with the normalized symbolic entropy:

$$u(\varepsilon) = -\frac{\sum_{k=0}^{n-1} p_k(\varepsilon) \log p_k(\varepsilon)}{n(\varepsilon)} \ , \tag{3}$$

where $p_k(\varepsilon)$ is the relative frequency of the symbol k, $n(\varepsilon)$ is the cardinality of the alphabet (number of states). Here, we divide the entropy by the cardinality of the alphabet in order to compensate for the influence of the alphabet size.

The second model rests upon the following assumptions about the ideal system's dynamics. (i) The system's states exhibit mainly self-transitions, i.e., transition probabilities p_{ii} are larger than the probabilities of other transitions. (ii) There are no direct transitions from one metastable state to another without passing through transient state, i.e., $p_{ij} = 0$ when $i \neq j$ for $i, j > 0$. (iii) Probabilities of transitions from and to transient states, p_{0i} and p_{i0}, respectively, are distributed according to the principle of maximum entropy. We can now construct a transition matrix corresponding to the desired dynamics:

$$\boldsymbol{P} = \begin{bmatrix} 1-(n-1)q & r & r & \cdots & r \\ q & 1-r & 0 & \cdots & 0 \\ q & 0 & 1-r & \cdots & 0 \\ \vdots & \vdots & \vdots & \ddots & \vdots \\ q & 0 & 0 & \cdots & 1-r \end{bmatrix} \ , \tag{4}$$

here, the total number of states is n and the number of recurrence states is $n-1$, diagonal elements correspond to the probabilities of self transitions, $q = p_{i0}$ and $r = p_{0i}$ for $i, j > 0$ are transition probabilities to and from transient state $s_0 = 0$.

Keeping in mind the three criteria of the optimal dynamics, we can achieve the desired utility function by: (i) maximizing the trace of the transition matrix $\operatorname{tr} \boldsymbol{P} = 1 + (n-1)(1-q-r)$; (ii) maximizing the normalized entropy of transition

probabilities of the first row and the first column of $\boldsymbol{P}$ after neglecting p_{00}, i.e., $p'_{0i} = p_{0i}/\sum_{i=1}^{n-1} p_{0i}$ for the first row and $p'_{i0} = p_{i0}/\sum_{i=1}^{n-1} p_{i0}$ for the first column. (iii) suppressing transitions between recurrence states by simultaneously maximizing the trace and the entropies of the first row and column of $\boldsymbol{P}$, due to normalization condition $\sum_{i=0}^{n-1} p_{ij} = 1$. Then the utility function is given by:

$$u(\varepsilon) = \frac{1}{n-2}\Big(\text{tr } \boldsymbol{P}(\varepsilon) + h_r(\varepsilon) + h_c(\varepsilon)\Big) \ , \tag{5}$$

where h_r and h_c are the entropies of the first row and column of $\boldsymbol{P}$ (see [12] for more details).

2.2 Phase Space Reconstruction

A dynamical system is defined by an evolution law in a phase space. This space is d-dimensional, where each dimension correspond to a certain property of a system (for instance, position, and velocity). Each point of the phase space refers to a possible state of the system. An evolution law, which is normally given by a set of differential equations, defines system's dynamics, shown as a trajectory in a phase space.

In certain cases only discrete measurements of a single observable are available, in this situation a phase space should be reconstructed according to Takens's theorem [26], which states that phase space presented with a d-dimensional manifold can be mapped into $2d+1$-dimensional Euclidean space preserving dynamics of the system. Several method of phase space reconstruction exist: delay embedding [26], numerical derivatives [23] and others (see for instance [16]).

In this work we propose a new method of phase space reconstruction based on the time-frequency representation of a signal. A time-frequency representation (TFR) is a distribution of the power of the signal over time and frequency. Here, the power in each frequency band contributes to a dimension of the reconstructed phase space. This approach is well-adapted for non-stationary and, especially, for oscillatory data, allowing better detection of oscillatory components rather than creating RPs point-wise from the signal. In this article we compare performance of the SRSA with different reconstruction methods, delay embedding and two different TFRs: spectrogram and scalogram.

Delay embedding. Assume, we have a time series which represents scalar measurements of a system's observable in discrete time:

$$x_n = x(n\Delta t), \quad n = 1, \ldots, N \ , \tag{6}$$

where Δt is measurement sampling time. Then reconstructed phase space is given by:

$$\boldsymbol{s}_n = \big[x_n, x_{n+\tau}, x_{n+2\tau}, \ldots, x_{n+(m-1)\tau}\big], \quad n = 1, \ldots, N - (m-1)\tau \ , \tag{7}$$

where m is the embedding dimension and τ is the time delay.

These parameters play an important role in correct reconstruction and should be estimated appropriately. Optimal time delay τ should be chosen such that delay vectors from (7) are sufficiently independent. The most common technique to correctly estimate the τ parameter is based on average mutual information [8, 19]. Moreover, the main attribute of appropriately chosen dimension m is that the original d-dimensional manifold will be embedded into an m-dimensional space without ambiguity, i.e., self-crossing and intersections. We apply the method of false nearest neighbors [15], which permits the estimation of the minimal embedding dimension.

Time-Frequency Representation. Time-frequency representation of a signal shows the signal's energy distribution in time and frequency. In this work we analyze two different types of TFR: the spectrogram and the scalogram (based on continuous wavelet transform).

The spectrogram $S^h(t, \omega)$ of a signal $x(t)$ is the square magnitude of its short-time Fourier transform (STFT):

$$X_h(t, \omega) = \int\limits_{-\infty}^{+\infty} x(\tau) h^*(t - \tau) \mathrm{e}^{-i\omega\tau}\, \mathrm{d}\tau \ , \tag{8}$$

where $h(t)$ is a smoothing window and $*$ denotes the complex conjugate, i.e., $S_h(t, \omega) = |X_h(t, \omega)|^2$.

The continuous wavelet transform (CWT) [1] is obtained by convolving the signal with a set of functions $\psi_{ab}(t)$ obtained by translation and dilation of a mother wavelet function $\psi_0(t)$:

$$T_\psi(b, a) = \frac{1}{\sqrt{a}} \int\limits_{-\infty}^{+\infty} x(t) \psi_0^* \left(\frac{t - b}{a} \right) \mathrm{d}t \ , \tag{9}$$

then, by analogy with the spectrogram, the squared magnitude of the CWT is called scalogram: $W_\psi(b, a) = |T_\psi(b, a)|^2$. In practice, the scale a can be mapped to a pseudo-frequency f and the dilation b represents a time instance and hence the time-frequency distribution is given by $W_\psi(t, f)$.

The scalogram was computed using analytical Morlet wavelet, and a Hamming window with 80% overlap was chosen for the spectrogram. In all the methods the window length and scale locations were chosen such as to achieve a frequency resolution of 0.2Hz for synthetic data and 1Hz for experimental data.

2.3 Complexity Measure

To quantitatively assess the obtained symbolic sequences we propose to measure its complexity. We present here three different complexity measures. These are the cardinality of the sequence's alphabet and the number of distinct words obtained from the sequence [13], where a word is a unique group of the same

symbols. In addition, we compute the well-known Lempel-Ziv (LZ) complexity [18], which is related to the number of distinct substrings and the rate of their occurrence along the symbolic sequence. All of the complexity measures have in common the notion of complexity, that is the number of distinct elements required to encode the symbolic string. The more complex the sequence is, the more of such elements are needed to present it without redundancy.

To demonstrate these measures we generated 100 artificial signals of two kinds (see below) with random initial conditions and random noise.

2.4 Synthetic Data

Transient Oscillations. The signal is a linear superposition of three signals, which exhibit sequences of noisy transient oscillations at a specific frequency [27]. These frequencies are 1.0 Hz, 2.25 Hz and 6.3 Hz, cf. Fig. 1a. The sampling frequency is 50 Hz and the signal has a duration of 70 s. Figure 1 shows the three different transient oscillations whose sum represents the signal under study.

Lorenz System. The solution of the chaotic Lorenz system [20, 11] exhibits two wings which are approached in a unpredictable sequence. These wings represent metastable signal states. Figure 1b shows the time series of the z-component of the model.
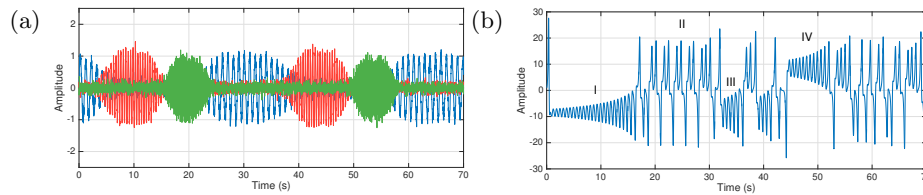

Fig. 1. Example signals of the synthetic data. (a) Three signals, whose sum represents the transient oscillation signal under study. (b) Solution of the Lorenz system along a single dimension.

2.5 Experimental Data

We examine electroencephalographic data (EEG) obtained during surgery under general anesthesia [25]. The EEG data under investigation has been captured at frontal electrodes 2 minutes before (pre-incision phase) and 2 minutes after (post-incision phase) skin incision and last 30 seconds. The raw signal was digitized at a rate of 128 Hz and digitally band-pass filtered between 1 Hz and 41 Hz using a 9th order Butterworth filter. The question in the corresponding previous study [25] was whether it is possible to distinguish the pre-incision from post-incision phase just on the basis of the captured EEG time series.

3 Results

3.1 Synthetic data

Time-Frequency Embedding. To illustrate the method, Fig. 2 (see also [7]) shows two different time-frequency representations of the transient oscillations signal. Spectrogram yields time-frequency intervals of high power at very good accordance with the underlying dynamics, cf. Sect. 2.4. In contrast, wavelet analysis smears out upper frequencies as a consequence of their intrinsic normalization of power. The symbolic sequences and the corresponding recurrence plots (middle and right-hand side of the panel) derived from the spectrogram fits perfectly to the underlying dynamics and are the same for both utility functions. They exhibit three different symbols in the symbolic sequence color-coded in blue, red and orange separated be transient states (color-coded in beige) in Fig. 2a and alternate in very good accordance to the three different transient oscillations. They are also visible as three rectangles of different size in the symbolic recurrence plot. Conversely, the scalogram yield only two recurrent signal features (entropy) and few recurrent states of brief duration (Markov), which do not reflecting the underlying dynamics.
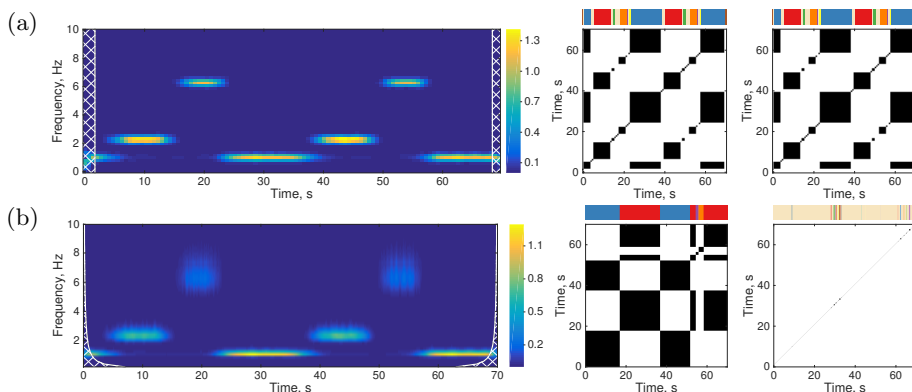

Fig. 2. Results for the transient oscillation signal. (a) Spectrogram; (b) scalogram. On each subfigure, left: time-frequency representation, middle: RPs with corresponding symbolic sequences above them (entropy utility function), right: the same but with Markov utility function. In each symbolic sequence colors denote metastable states and transient states show in beige.

Typically experimental neurophysiological signals exhibit a less regular temporal structure than given in the transient oscillations example. Solutions of the Lorenz system exhibit chaotic behavior, that is rather irregular and exhibits metastable oscillatory states. Since experimental EEG may exhibit chaotic behavior [10, 9], the Lorenz signal is tentatively closer to neurophysiological data. Figure 3 shows the TFR of the Lorenz signal. For both TFRs, one can well

identify visually the four signal states I to IV marked in Fig.1b. The color-coded symbolic sequences extracted from the spectrogram (seen in Fig.3a) identify correctly the time windows of the signal states I to IV and are identical for both utility functions. The states I, II and IV are well captured, whereas the short state III is not well identified. The scalogram results are much worse in case of entropy utility function only states I and IV are identified, while Markov utility function captures all four states but no recurrence is present.
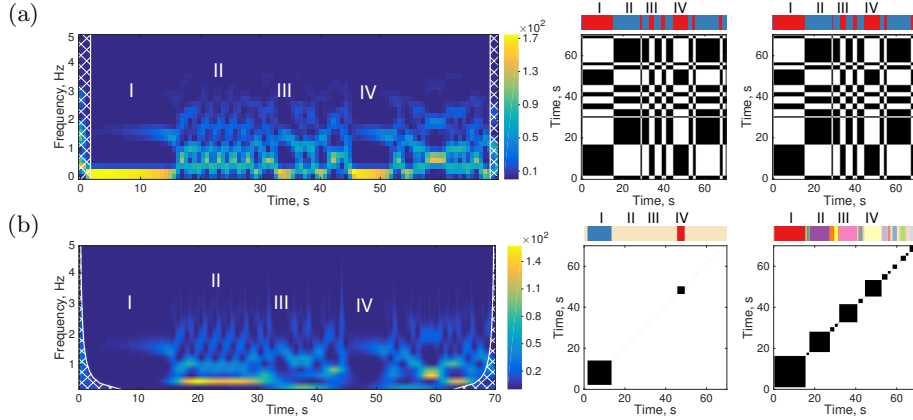

Fig. 3. Results for the Lorenz system. (a) Spectrogram; (b) scalogram. On each subfigure, left: time-frequency representation, middle: RPs with corresponding symbolic sequences above them (entropy utility function), right: the same but with Markov utility function. In each symbolic sequence colors denote metastable states and transient states show in beige.

Delay Embedding. To illustrate the power of the method proposed, we compare our results to recurrence analysis results utilizing delay embedding, cf. Sect. 2.2. We consider the transient oscillations and the Lorenz signal, compute the optimal delay embedding parameters and apply the recurrence analysis technique to gain the symbolic sequences and the recurrence plots. Figure 4 (see also [7]) reveals that the delay embedding essentially fails in detecting the recurrence domains in the transient oscillations compared to the time-frequency embedding (in case of both utility functions). In the Lorenz signal all states I-IV are captured in the symbolic sequence and visible in the recurrence plot, however the detection is much worse than with time-frequency embedding, cf. Fig. 3. Also entropy utility function tends to produce few recurrent states with no transient states, whilst the usage of the Markov utility entails larger numbers of metastable and transient states.
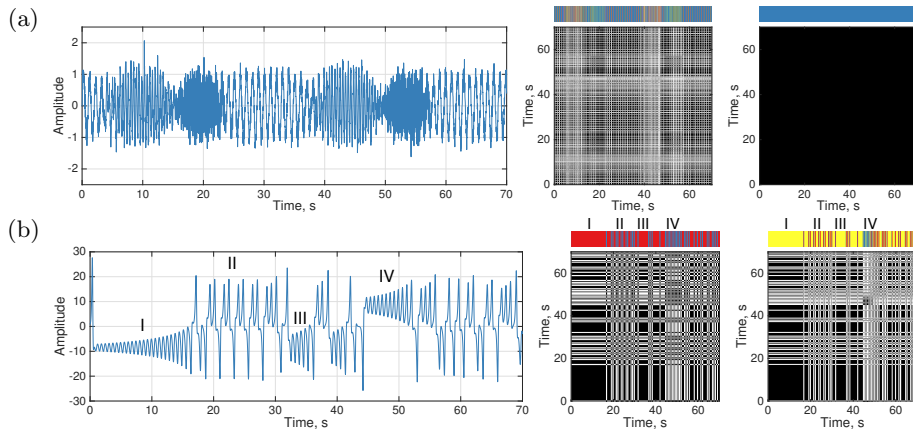
Fig. 4. Results obtained with delay embedding. (a) The transient oscillations, reconstruction parameters: $m = 5$, $\tau = 0.1$ s; (b) the Lorenz system, reconstruction parameters: $m = 3$ and $\tau = 0.16$ s.

Complexity Measures. To quantify the intrinsic temporal structure, in addition we compute three complexity measures for each of the signals. To demonstrate the ability of complexity measures to distinguish temporal structures, Fig. 5 gives the distribution of complexity measures for both artificial datasets. We show results obtained with spectrogram, however the results for other embeddings are similar (not shown here for the sake of brevity). We observe that all complexity measures show significantly different distributions. Qualitatively, the largest difference between both signals is reflected in the LZ complexity measure. We also observe that in general complexities of Lorenz system are larger than the ones of transient oscillations when obtained with Markov utility, it is the opposite for entropy utility function.
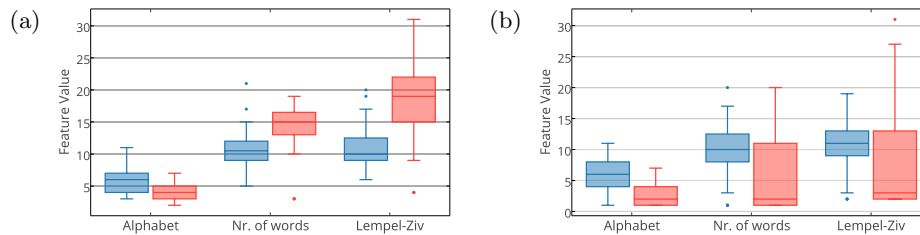

Fig. 5. Boxplots of three complexity measures for transient oscillations (blue) and Lorenz system (red) obtained with the spectrogram. (a) Entropy utility function; (b) Markov utility function. For each complexity measure, both distributions are significantly different (Kolmogorov-Smirnov test with $p < 0.001$).

3.2 EEG data

Finally, we study experimental EEG data. Figure 6 shows time-frequency plots (spectrogram) with corresponding symbolic sequences for two patients before and after incision during surgery. We observe activity in two frequency bands, namely strong power in the δ-band $(1-5$ Hz$)$ and lower power in the α-range $(8-12$ Hz$)$. This finding is in good accordance to previous findings in this EEG dataset [25]. The corresponding spectral power is transient in time in both frequency bands, whose temporal structure is well captured by the recurrence analysis with entropy utility function as seen in the symbolic sequences. The symbolic analysis with Markov utility function captures underlying dynamics well in case of patient #1099 (post-incision). In general Markov-based recurrence analysis tends to extract less recurrence domains separated by long transitions.
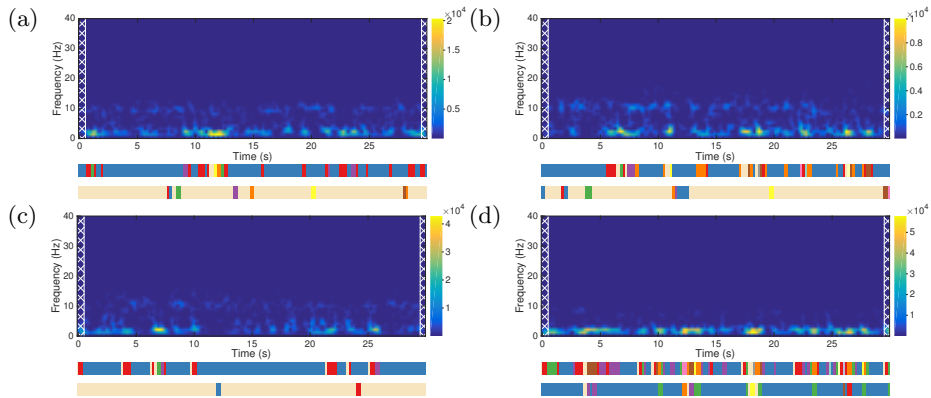

Fig. 6. Results for EEG signals obtained with spectrogram. Two colorbars below represent symbolic sequences obtained with entropy utility function (top) and Markov utility function (bottom). In each symbolic sequence colors denote metastable states and transient states show in beige.(a) Patient #1065 (pre-incision); (b) Patient #1065 (post-incision); (c) Patient #1099 (pre-incision); (d) Patient #1099 (post-incision).

In order to characterize the temporal structure, we compute the symbolic sequences' recurrence complexity, which are shown in Table 1. We observe that the values of the various complexity measures are very similar in pre- and post-incision data and close between patients. However complexities obtained with entropy utility function reveal larger differences between experimental conditions than between patients, whilst Markov utility function demonstrates larger variation between patients than between the conditions. Since the time periods of pre- and post-incision data are captured several minutes apart and hence the corresponding data are uncorrelated, their similarity of complexity measures is remarkable pointing out to a constant degree of complexity in each patient. This is in line with the different complexity measures in both patients indicating different complexity measures.

Complexity measure	Entropy		Markov	
	Pre-incision	Post-incision	Pre-incision	Post-incision
Patient #1065				
Alphabet size	7	12	8	9
Nr. of words	19	25	15	12
Lempel-Ziv	22	27	13	13
Patient #1099				
Alphabet size	5	13	3	8
Nr. of words	15	28	5	20
Lempel-Ziv	16	40	6	20

Table 1. Complexity measures of EEG signals (spectrogram).

4 Discussion

The present work shows that recurrence analysis can be employed on univariate time series if, at first, the data is transformed into its time-frequency representation. This transform provides a multivariate time series whose number of dimensions is equal to the number of frequency bins considered. We show that the best time-frequency representation for the synthetic time series is the spectrogram. We compare two approaches for estimation of optimal threshold distance required in SRSA. We demonstrate that a model of system's dynamics can be easily incorporated in the method through a utility function. However, if the model is not accurate the performance is worse. The recurrence structures extracted can be represented by a symbolic sequence whose symbolic complexity may serve as an indicator of the time series complexity. The EEG data analysis performed in this study indicates that the symbolic complexity may serve as a classifier to distinguish temporal structures in univariate time series.

References

1. Addison, P.S.: The Illustrated Wavelet Transform Handbook: Introductory Theory and Applications in Science, Engineering, Medicine and Finance. Inst. of Physics Publ, Bristol, UK; Philadelphia (2002)
2. Allefeld, C., Atmanspacher, H., Wackermann, J.: Mental states as macrostates emerging from EEG dynamics. Chaos 19, 015102 (2009)
3. beim Graben, P., Hutt, A.: Detecting event-related recurrences by symbolic analysis: applications to human language processing. Philos Trans A Math Phys Eng Sci 373(2034) (2015)
4. Donner, R., Hinrichs, U., Scholz-Reiter, B.: Symbolic recurrence plots: A new quantitative framework for performance analysis of manufacturing networks. Eur. Phys. J. Spec. Top. 164(1), 85–104 (2008)
5. Eckmann, J.P., Kamphorst, S.O., Ruelle, D.: Recurrence Plots of Dynamical Systems. Europhys. Lett. EPL 4(9), 973–977 (1987)

6. Faure, P., Lesne, A.: Recurrence plots for symbolic sequences. Int. J. Bifurc. Chaos 20(06), 1731–1749 (2010)
7. Fedotenkova, M., beim Graben, P., Sleigh, J., Hutt, A.: Time-Frequency Representations as Phase Space Reconstruction in Recurrence Symbolic Analysis. In: Valenzuela, O., Rojas, F., Ruiz, G., Pomares, H., Rojas, I. (eds.) Proceedings ITISE 2016. p. 850. Granada, Spain (2016)
8. Fraser, A.M., Swinney, H.L.: Independent coordinates for strange attractors from mutual information. Phys. Rev. A 33(2), 1134–1140 (1986)
9. Freeman, W.J.: Evidence from human scalp EEG of global chaotic itinerancy. Chaos 13(3), 1069 (2003)
10. Friedrich, R., Uhl, C.: Spatio-temporal analysis of human electroencephalograms: Petit-Mal epilepsy. Phys. D 98, 171–182 (1996)
11. beim Graben, P., Hutt, A.: Detecting recurrence domains of dynamical systems by symbolic dynamics. Phys. Rev. Lett. 110(15), 154101 (2013)
12. beim Graben, P., Sellers, K.K., Fröhlich, F., Hutt, A.: Optimal estimation of recurrence structures from time series. EPL 114(3), 38003 (2016)
13. Hu, J., Gao, J., Principe, J.C.: Analysis of biomedical signals by the Lempel-Ziv Complexity: the effect of finite data size. IEEE Trans. Biomed. Eng. 53(12), 2606–2609 (2006)
14. Hutt, A., Riedel, H.: Analysis and modeling of quasi-stationary multivariate time series and their application to middle latency auditory evoked potentials. Phys. D 177, 203–232 (2003)
15. Kennel, M.B., Abarbanel, H.D.I.: False neighbors and false strands: A reliable minimum embedding dimension algorithm. Phys. Rev. E 66(2), 026209 (2002)
16. Kugiumtzis, D., Christophersen, N.D.: State space reconstruction: method of delays vs singular spectrum approach. Res. Rep. Httpurn Nb NoURN NBN No-35645 (1997)
17. Larralde, H., Leyvraz, F.: Metastability for Markov processes with detailed balance. Phys. Rev. Lett. 94(16), 160201 (2005)
18. Lempel, A., Ziv, J.: On the complexity of finite sequences. IEEE Trans. Inf. Theory 222(1), 75–81 (1976)
19. Liebert, W., Schuster, H.G.: Proper choice of the time delay for the analysis of chaotic time series. Phys. Lett. A 142(2), 107–111 (1989)
20. Lorenz, E.N.: Deterministic nonperiodic flow. J. Atmos. Sci. 20(2), 130–141 (1963)
21. Marwan, N., Kurths, J.: Line structures in recurrence plots. Phys. Lett. A 336, 349–357 (2005)
22. Marwan, N., Romano, M.C., Thiel, M., Kurths, J.: Recurrence plots for the analysis of complex systems. Phys. Rep. 438(5–6), 237–329 (2007)
23. Packard, N.H., Crutchfield, J.P., Farmer, J.D., Shaw, R.S.: Geometry from a time series. Phys. Rev. Lett. 45(9), 712 (1980)
24. Poincaré, H.: Sur le problème des trois corps et les équations de la dynamique. Acta Math. 13(1), 3–270 (1890)
25. Sleigh, J.W., Leslie, K., Voss, L.: The effect of skin incision on the electroencephalogram during general anesthesia maintained with propofol or desflurane. J. Clin. Mon. Comput. 24, 307–318 (2010)
26. Takens, F.: Detecting strange attractors in turbulence. Springer (1981)
27. Tošić, T., Sellers, K.K., Fröhlich, F., Fedotenkova, M., beim Graben, P., Hutt, A.: Statistical frequency-dependent analysis of trial-to-trial variability in single time series by recurrence plots. Fronti. Syst. Neurosci. 9(184) (2016)
28. Yildiz, I.B., Kiebel, S.J.: A hierarchical neuronal model for generation and online recognition of birdsongs. PLoS Comput. Biol. 7, e1002303 (2011)